SEMARAK ILMU PUBLISHING

CFD Letters

Journal homepage:
https://semarakilmu.com.my/journals/index.php/CFD_Letters/index
ISSN: 2180-1363

Study of Hydrodynamics and Upscaling of Immiscible Fluid Stirred Tank using Computational Fluid Dynamics Simulation

Ekaroek Phumnok[1], Waritnan Wanchan[2], Matinee Chuenjai[2], Panut Bumphenkiattikul[3,4], Sunun Limtrakul[5], Sukrittira Rattanawilai[1], Parinya Khongprom[1,6,*]

[1] Department of Chemical Engineering, Faculty of Engineering, Prince of Songkla University, Songkhla 90110, Thailand
[2] Department of Industrial Chemistry, Faculty of Applied Science, King Mongkut's University of Technology North Bangkok, Bangkok 10800, Thailand
[3] Simulation Technology, Digital Manufacturing, Chemicals Business, SCG, 1 Siam Cement Road, Bang sue, Bangkok 10800, Thailand
[4] The Thai Institute of Chemical Engineering and Applied Chemistry, Department of Chemical Engineering, Faculty of Engineering, Chulalongkorn University, Bangkok 10330, Thailand
[5] Department of Chemical Engineering, Faculty of Engineering, Kasetsart University, Jatujak, Bangkok 10900, Thailand
[6] Air Pollution and Health Effect Research Center, Prince of Songkla University, Songkhla 90110, Thailand

ARTICLE INFO

Article history:
Received 7 may 2022
Received in revised form 3 June 2022
Accepted 7 June 2022
Available online 30 June 2022

Keywords:
Immiscible liquid-liquid stirred tank; Computational fluid dynamics; Scale up; Hydrodynamic; Mixing time

ABSTRACT

Stirred tanks are prevalent in various industries, including chemical, biochemical, and pharmaceutical industries. These reactors are suitable for ensuring efficient mass and heat transfer because adequate mixing can be achieved. Numerous studies have been conducted on small-scale stirred-tank reactors. However, upscaling such reactors is challenging because of the complex flow behavior inside the system, especially for the mixing of immiscible liquid–liquid systems. Thus, the objectives of this study were to examine the flow behavior and upscale an immiscible liquid–liquid stirred tank using CFD simulation by investigating a flat-bottomed stirred tank reactor, equipped with a six-blade Rushton turbine. The simulated results were in good agreement with those obtained experimentally. The scale of the reactor significantly affects the hydrodynamic behavior, and the uniformity of the radial distribution of the velocity decreases with increasing Reynolds number. Furthermore, the upscaling criteria were evaluated for geometric similarity and equal mixing times. The proposed scaling law reliably scaled up the immiscible liquid–liquid mixing in a stirred tank with a difference in the range of ±10%.

1. Introduction

Stirred tank reactors are widely utilized in industry and are crucial for manufacturing various products. The stirred tank reactor works as a mixer, wherein the material is mixed using an impeller, thereby improving the mass and heat transfer. Consequently, the reaction is enhanced. Additionally, the stirred tank reactor is suitable for mixing multi-phase systems, such as solid–liquid, solid–liquid–

* *Corresponding author.*
E-mail address: parinya.kh@psu.ac.th (Parinya Khongprom)

https://doi.org/10.37934/cfdl.14.6.115133

gas, and liquid–liquid, wherein flow characteristics are commonly differentiated and complicated. Immiscible liquid–liquid dispersions are relevant in several applications in the chemical, pharmaceutical, food, polymerization, and petroleum sectors [1]. Dispersion is hindered due to the occurrence of several phenomena, such as the interaction of continuous and dispersed phases, dynamics of droplet characteristics, and presence of small amounts of impurities [2].

The flow characteristics of continuous and scattered phases of the immiscible liquid were studied. Distinct dispersion regimes occurring in tanks were observed by varying the impeller speeds [3, 4]. Furthermore, the agitation speed required for complete liquid–liquid dispersion was investigated [5-7]. In addition, the impeller configurations and physical properties of fluids, including viscosity, density, fluid ratio within the system, and surface tension, were considered for studying the flow characteristics [8-13]. However, the flow characteristics in immiscible liquid–liquid stirred tanks are still not completely understood.

Effective upscaling of immiscible liquid–liquid stirred tank is not easily achieved, owing to significant alterations in the flow behavior at the reactor scale. Several upscaling criteria have been proposed for stirred tanks based on the similarities in geometries, dynamics, and kinematics [14, 15]. Generally, four upscaling criteria are considered: equal power input per unit mass and geometric similarity; equal average circulation time and geometric similarity; equal power input per unit mass, equal averaged circulation time, and no geometric similarity; equal impeller tip speed and geometric similarity. The selection of upscaling criteria depends on the purpose of the study. In chemical reaction systems, the degree of mixing significantly influences the chemical performance. The mixing time should correlate with the reaction time to ensure a high reaction conversion. Thus, the mixing time is a suitable criterion for the scale-up of a stirred tank with a chemical reaction.

2. Methodology

2.1 Reactor Geometry

A flat-bottomed stirred tank reactor equipped with four baffles was considered in this study. The configuration is shown in Figure 1. The diameter and the height of the stirred tank are 0.14 and 0.28 m, respectively. A Rushton turbine impeller equipped with six blades was used. Each blade is 0.094 m wide and 0.0175 m long, as illustrated in Figure 1(b). The detailed configuration and installation of the stirred tank can be found in the existing literature [16]. The size of the upscaled stirred tank was thrice that of the original. The similarity of the reactors was determined using Eq. (1),

$$\frac{3}{1} = \frac{T_L}{T_S} = \frac{D_L}{D_S} = \frac{H_L}{H_S} \tag{1}$$

The configurations of the small and large stirred tanks are illustrated in Figure 2. The immiscible liquid–liquid mixing of silicone oil as hydrophobic phase and solution of sodium iodide (NaI) as aqueous phase was investigated. The NaI solution was prepared by dissolving of solid NaI in water. The physical properties of NaI solution and silicone oil employed in this study are identical to those of Svensson and Rasmuson's experimental study [16]. The densities of the NaI solution and the silicone oil are 1.34 and 0.94 g/cm^3, respectively; their viscosities are 1.4 and 11.0 mPa•s, respectively.

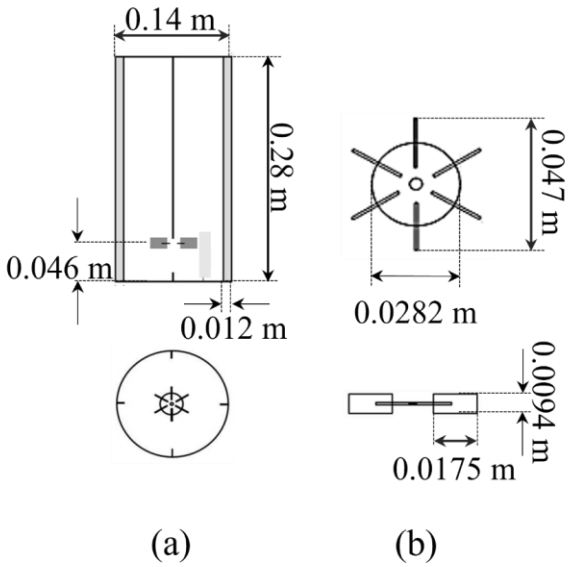

Fig. 1. Configurations of the stirred tank reactor (a), Rushton turbine agitator (b)

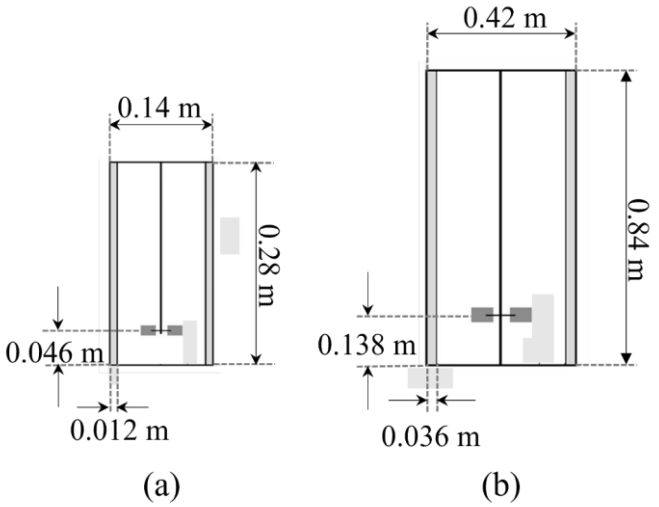

Fig. 2. Configurations of the small (a) and large (b) reactor tanks

2.2 Mathematical Model

In recent years, computational fluid dynamics (CFD) has been developed to solve the complex flow systems [17-22]. In this study, a two-fluid model based on the Eulerian–Eulerian approach was used to simulate flow behavior in a stirred tank. The following assumptions were considered: isothermal process, no mass transfer between phases, and no chemical reactions. Several forces affect the interphase momentum transfer, including the drag, added mass, lift, and Basset forces [23]. However, only the drag force was considered in this study because the other forces contribute minimally to interphase interactions [24-26]. The standard k–ε turbulence model was adopted to predict turbulent flow behavior [24, 27, 28]. The governing equations are presented as follows below.

The continuity equation is

$$\frac{\partial(\alpha_k\rho_k)}{\partial t}+\frac{\partial}{\partial x_i}\left(\alpha_k\rho_k u_{ki}+\rho_k\overline{\alpha_k^{'}u_k^{'}}\right)=0 \tag{2}$$

The momentum equation for the gas phase is given by

$$\frac{\partial(\alpha_k\rho_k u_{ki})}{\partial t}+\frac{\partial}{\partial x_i}\left(\alpha_k\rho_k u_{ki}u_{kj}\right) = -\alpha_k\frac{\partial P}{\partial x_i}+\alpha_k\rho_k g_i+F_{ki}-\rho_k\frac{\partial}{\partial x_i}\left(\alpha_k\overline{u_{kl}^{'}u_{kJ}^{'}}+u_{ki}\overline{\alpha_k^{'}u_{kJ}^{'}}+u_{kj}\overline{\alpha_k^{'}u_{kl}^{'}}\right) \tag{3}$$

The Reynolds stresses, $\overline{u_{kl}^{'}u_{kJ}^{'}}$, is defined as

$$\overline{u_{kl}^{'}u_{kJ}^{'}} = -v_{kt}\left(\frac{\partial u_{ki}}{\partial x_j}+\frac{\partial u_{kj}}{\partial x_i}\right)+\frac{2}{3}k\delta_{ij} \tag{4}$$

The correlation of the velocity and holdup fluctuations, $\overline{\alpha_k^{'}u_{kJ}^{'}}$ is

$$\overline{\alpha_k^{'}u_{kJ}^{'}}=-\frac{v_{kt}}{\sigma_t}\frac{\partial\alpha_k}{\partial x_i} \tag{5}$$

In Eq. (3), term F_{ki}, denotes the momentum exchange between the continuous and scattered phases, which is a linear combination among several momentum exchange mechanisms. Three separate forces are frequently considered: drag (F_{drag}), added mass (F_{am}), and lift (F_{lift}). This equation can be used to depict the drag force between the dispersed and continuous phases.

$$F_{ci,\mathrm{drag}}=-F_{di,\mathrm{drag}}=\frac{3\rho_c\alpha_c\alpha_d C_D|\mathbf{u_d}-\mathbf{u_c}|(u_{di}-u_{ci})}{4d_d} \tag{6}$$

Schiller-Naumann drag model was used in this study.

$$C_D=\begin{cases}\frac{24}{Re_d}(1+0.15Re_d^{0.687}) & Re\le 1000\\ 0.44 & Re>1000\end{cases} \tag{7}$$

where

$$Re_d=\frac{\rho_c d_d|\mathbf{u_d}-\mathbf{u_c}|}{\mu_{c,\mathrm{lam}}} \tag{8}$$

and

$$d_d=10^{-2.316+0.672\alpha_d}v_{c,\mathrm{lam}}^{0.0722}\epsilon^{-0.914}\left(\frac{\sigma g}{\rho_c}\right)^{0.196} \tag{9}$$

The standard k-ε two equation turbulent model is obtained from

$$\frac{\partial}{\partial t}(\alpha_{\mathrm{c}}\rho_{\mathrm{c}}\emptyset)+\frac{\partial}{\partial x_i}(\alpha_{\mathrm{c}}\rho_{\mathrm{c}}u_{\mathrm{ci}}\emptyset)=\frac{\partial}{\partial x_i}\left(\alpha_{\mathrm{c}}\frac{\mu_{\mathrm{ct}}}{\sigma_{\emptyset}}\frac{\partial\emptyset}{\partial x_i}\right)+S_{\emptyset} \quad (10)$$

where Ø can be either k or ε and $\sigma_{\emptyset}$ is the model parameter describing turbulent dispersion of k

The turbulent viscosity of the continuous phase, μ_{ct}, is express as

$$\mu_{ct}=C_{\mu}\rho_{\mathrm{c}}k^2/\epsilon \quad (11)$$

The turbulent viscosity of the dispersed phase, μ_{dt}, is given by

$$\mu_{dt}=K\mu_{\mathrm{ct}} \quad (12)$$

A correlation of $u_{\mathrm{d}i}^{'}$ to $u_{\mathrm{c}i}^{'}$ is express as

$$u_{\mathrm{d}i}^{'}=u_{\mathrm{c}i}^{'}[1-\exp\left(-\frac{t_1}{t_p}\right) \quad (13)$$

where $t_1=0.41k/\epsilon$ is the mean eddy lifetime and t_p is the particle response time derived using Lagrangian integration of the motion equation of a swarm of droplets traveling through a fluid eddy using the expression

$$t_{\mathrm{p}}=\frac{4\rho_{\mathrm{d}}d_{\mathrm{d}}}{2\rho_{\mathrm{d}}\mathrm{C_D}\alpha_{\mathrm{d}}|\mathbf{u}_{\mathrm{d}}-\mathbf{u_c}|} \quad (14)$$

2.3 Numerical Solution

In this study, the hydrodynamic flow behavior of a three-dimensional liquid–liquid stirred tank was simulated using the commercial computational fluid dynamics (CFD) software Ansys Fluent. The governing equations were solved numerically using the finite volume method. The least-squares cell-based method was chosen for gradient discretization. First-order upwind schemes were defined discretizing turbulent kinetic energy, turbulent dissipation rate, momentum, and volume fraction. The semi-implicit pressure-linked equation (SIMPLE) algorithm was used for pressure and velocity coupling in the momentum equation. Multiple reference frames, widely used in previous research [29-32], were considered in this study. The wall boundary conditions of the tank, impeller, and baffles were set as the no-slip conditions. The agitation speed varied in the impeller and rotor regions.

2.4 Estimation of Mixing Time

The mixing time in a stirred tank can be investigated experimentally or numerically using the tracer method [33-35]. Several models and correlations have been proposed to estimate the mixing time [36]. The mixing time of miscible liquids (ethanol in glycerol) in semi-batch and batch stirred tanks was investigated using CFD simulations [37]. The degree of mixing was estimated using the viscosity of the liquid mixture and the ethanol mass fraction. In the batch reactor, two distinct layers of ethanol and glycerol were observed during the initial conditions. The liquid mixture viscosity and mass fraction of ethanol were investigated as a function of time at nine positions in the reactor. The

mixing time was obtained when all investigated points exhibited the same properties. The simulated mixing times were in good agreement with the experimental values. Thus, this concept was applied to estimate the mixing time of an immiscible liquid–liquid (silicone oil in NaI solution) stirred tank. At t = 0 s, silicone oil and NaI solution were filled in a stirred tank; two distinct layers were observed. The progress of mixing is determined from the contour of the silicone oil volume fraction as a function of time, as shown in Figure 3.

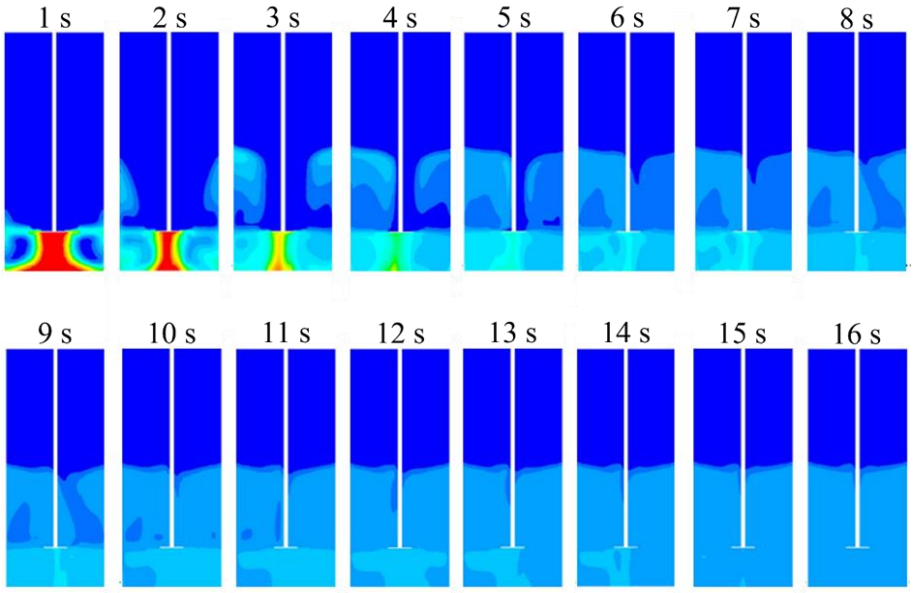

Fig. 3. The contour of the silicone oil volume fraction as a function of time

The mixing time is defined as the time at which the contour of the silicone oil volume fraction is uniformly distributed throughout the system. The mixing time is determined from the standard deviation (S. D.) of the silicone oil volume fraction in the system using Eq. (15),

$$S.D. = \sqrt{\frac{(x_i - \bar{x})^2}{n}} \tag{15}$$

where x_i is the volume fraction at position i; $\bar{x}$ is the average volume fraction; and n is the total number of data points. In this study, the volume fraction was investigated at different heights Z/H (0.1, 0.3, 0.5, and 0.7) and r/R positions (0.35 and 0.7), equivalent to 16 data point measurements, as shown in Figure 4. Figure 5 shows the distribution of the S. D. of the dispersed-phase volume fraction as a function of time. t95, representing 95% of the perfect uniformity, was considered the mixing time (t_{mix}).

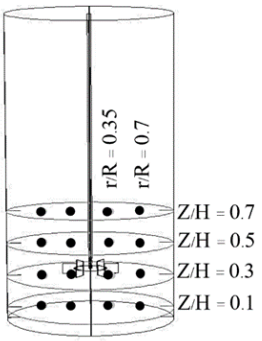

Fig. **4**. XZ-plane stirring tank reactor at height Z**/**H **=** 0**.**1, 0**.**3, 0**.**5 and 0**.**7

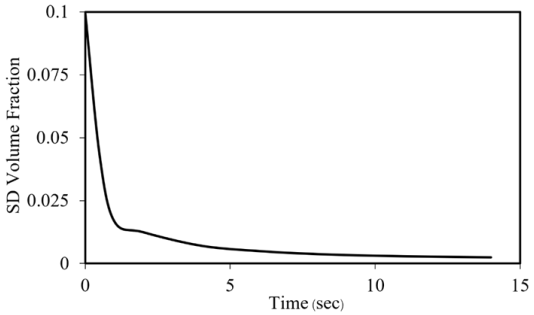

Fig. **5**. The distribution of the S**.**D**.** of disperse phase volume fraction as a function of time

3. Results and Discussion

3.1 Grid Sensitivity Study

Studying the grid size sensitivity is crucial for numerical investigation because the grid size significantly affects the accuracy of the CFD prediction. A fine grid results in a highly accurate answer but requires a long computational time, whereas a coarse grid requires a short calculation time but generates a considerable margin of error in the simulated results. Thus, the effect of grid size on the simulated results should be analyzed to obtain the optimum grid system. Four grid distributions were investigated with a varying number of cells: coarse (33,109 and 68,605), medium (94,961), and fine (191,647) grids—depicted in Figure 6.

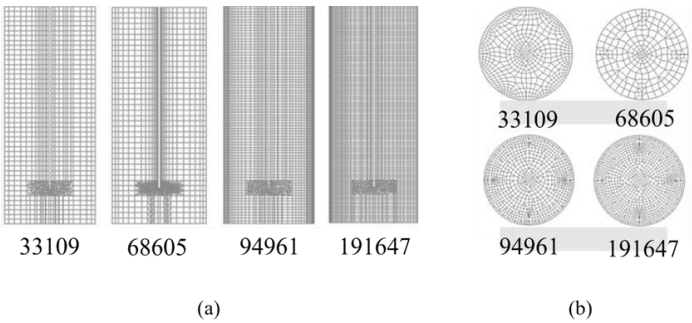

Fig. 6. Four different grid distributions of 33,109 (coarse), 68,605 (coarse), 94,961 (medium) and 191,647 (fine) grids at cross-section X-Y (a) and cross-section X-Z (b)

Figure 7 displays the radial distribution of the axial (a), radial (b), and tangential (c) velocities of the disperse phase for various grid distributions at heights of 10 and 103 mm from the bottom of the tank. The simulated results for all cases exhibit a similar trend. The differences between the simulated results obtained from the coarsest and finest grids are insignificant. Based on the accuracy and computational time, the optimum grid was the 94,961 grid system that was used for all subsequent simulations in this study.

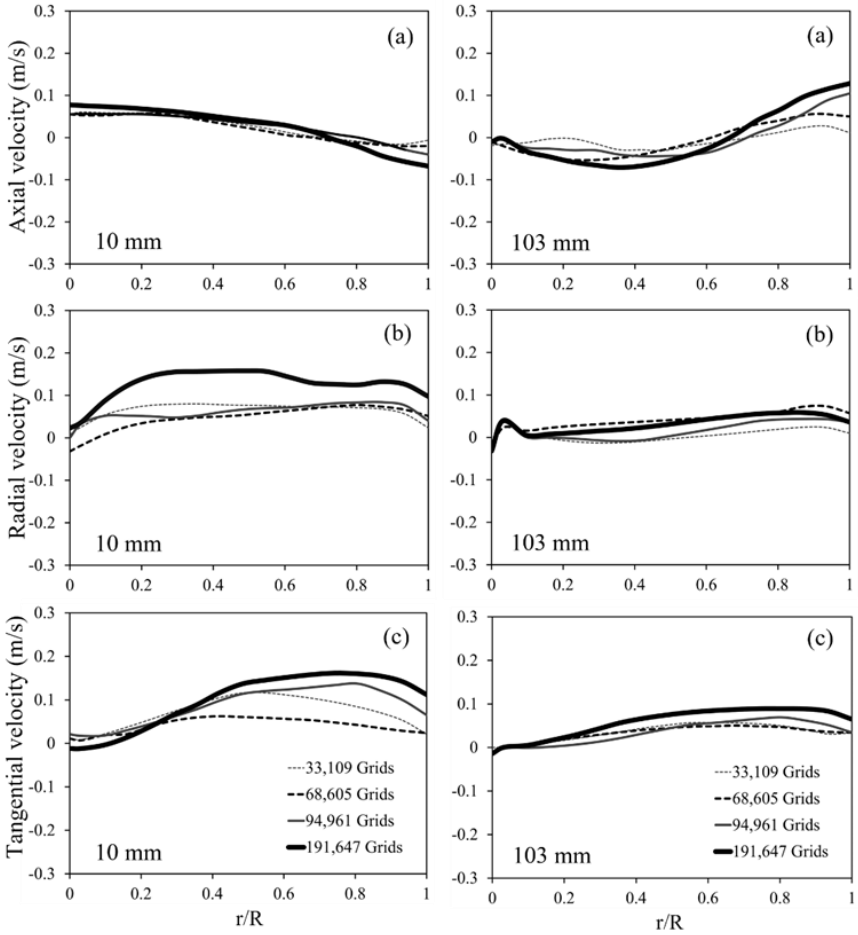

Fig. 7. The radial distribution of the axial velocity (a), the radial velocity (b), and the tangential velocity (c) of the disperse phase for various grid distributions at the heights of 10 and 103 mm from the tank bottom

3.2 Model Validation

The model was initially validated by comparing the velocity distribution obtained from the CFD simulation with that of the experimental results based on laser doppler anemometry (LDA) [16]. Figure 8 shows a comparison of the axial, radial, and tangential velocities versus the radius of the reactor obtained from the simulation with experimental data at 540 rpm and 10% dispersed phase. The simulated results reasonably agree with the experimental data.

The dispersed-phase volume fraction is validated in Figure 9, wherein the simulated results are compared with those experimentally obtained by Wang and Mao (2005) [24]. The simulated results qualitatively and quantitatively exhibit the same trend as those of the experiment. An almost uniform distribution is observed, indicating a good dispersion of the silicone oil in the system.

Tip velocity, a critical characteristic that influences reactor performance, is defined as the velocity of the fluid at the impeller tip. Theoretically, it is calculated from the angular velocity and radius (R) of the agitator, as shown in Eq. (16)

$$V_{tip} = 2\pi NR \tag{16}$$

where N is the agitator speed. In addition, this term can be directly measured from the velocity of the fluid near the impeller tip.

Figure 10 shows the parity plot of the tip velocity obtained from simulations and calculations, exhibiting good quantitative agreement of the tip velocities. In summary, the results from the CFD simulation correspond well with the experimental data.

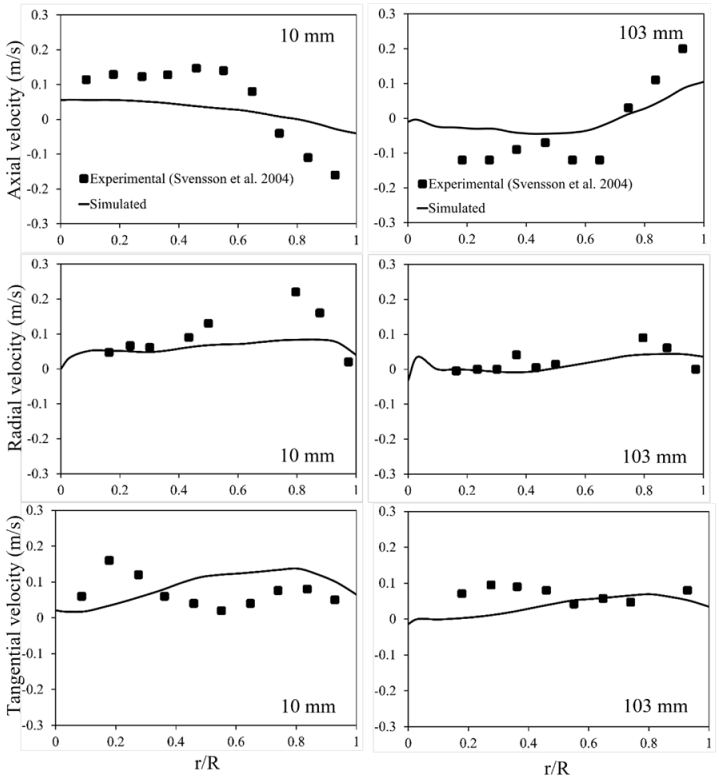

Fig. 8. A comparison of the axial, radial, and tangential velocities versus the radius of the reactor obtained from the simulation with the experimental data under 540 rpm and 10% dispersed phase

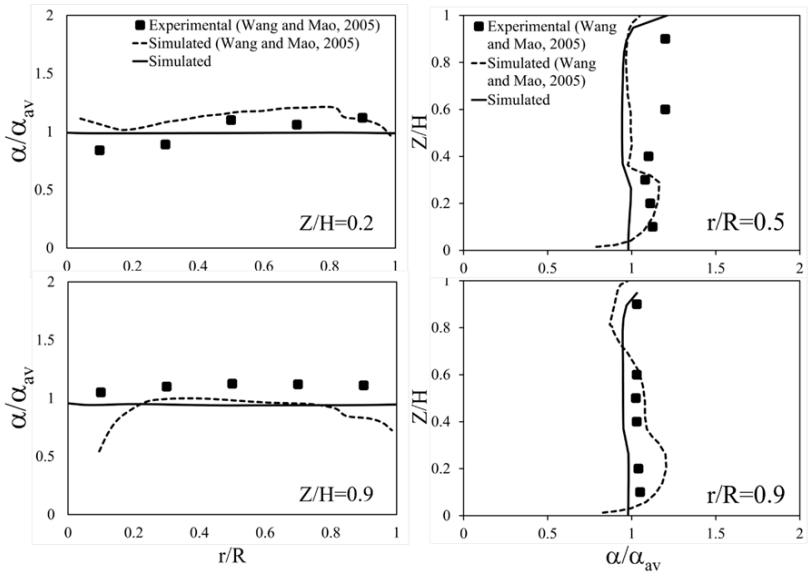

Fig. 9. The axial and radial variations of dispersed-phase holdup between simulation and experimental data

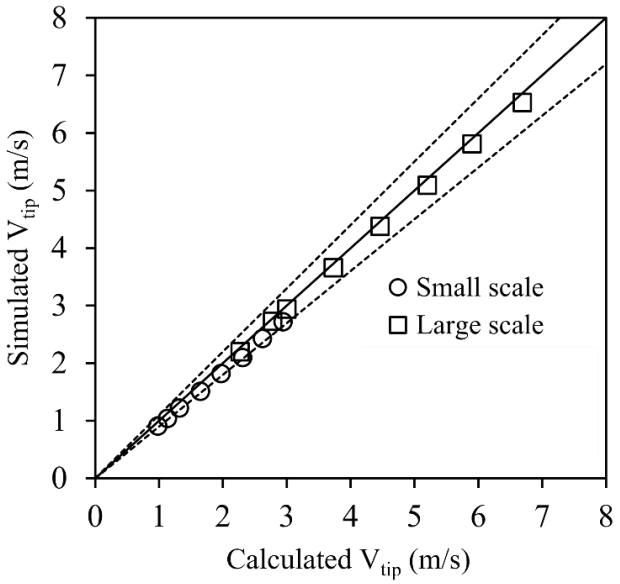

Fig. 10. The tip velocity obtained from simulations and calculated

3.3 Flow Behavior

The flow behavior within the stirred tank reactor can be used to efficiently optimize reactor design and operation. Figure 11 shows velocity vector plots of the continuous and dispersed phases, with both phases exhibiting identical flow patterns. The fluid moves rapidly from the tip of the agitator in a direction perpendicular to the shaft axis (radial direction) before divided into two zones at the tank wall. A portion of the liquid flows upward, circulated to the agitator (region above the agitator blade), while another portion flows downward and returned to the agitator (under the agitator blade). These flow characteristics are consistent with the radial flow pattern of a Rushton turbine agitator, which has also been observed in previous studies [7, 24, 38].

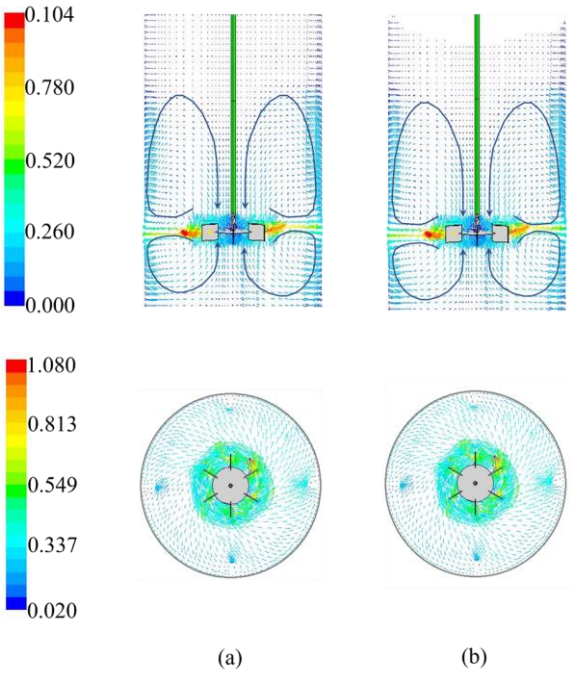

Fig. 11. The velocity vector plot of continuous (a) and disperse phases (b)

Figure 12 displays the contour plot of the steady-state dispersed-phase volume fraction for the small (a) and large (b) stirred tanks at various Reynolds numbers. The agitator speeds are in the range of 400–1100 rpm (Reynolds number = 8,000–24,500) and 310–910 rpm (Reynolds number = 50,000–150,000) for the small and large stirred tanks, respectively. All cases exhibit two blue-colored regions in the upper zone, representing the free space (without liquid in this region), and a sky-blue region in the lower part, representing the liquid layer region. A uniform color distribution is observed in the liquid region, indicating a uniform distribution of the dispersed phase in the liquid mixture. However, a vortex is observed (dark sky-blue contour around the shaft of the agitator) when operating under a high Reynolds number.

Figure 13 shows the velocity vector plot of the dispersed phase at steady state for the small and large stirred tanks. All cases exhibit a radial flow pattern with a high radial velocity in the cross-sectional area of the agitator. As expected, the velocity increases with increasing agitation speed. Figure 12 shows the contour plot of the velocity corresponding to Figure 13. Evidently, the velocity increases with increasing Reynolds number.

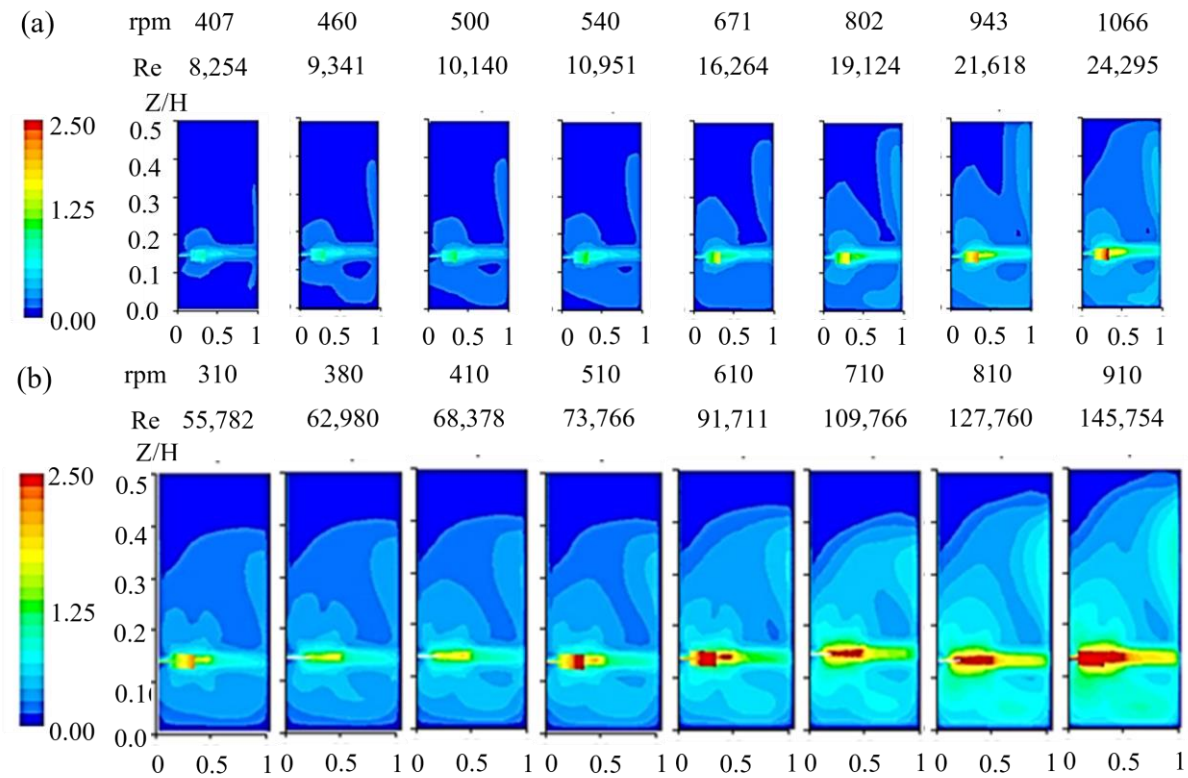

Fig. 12. The contour plot of the dispersed phase volume fraction at the steady state of the small (a) and large (b) stirred tanks under various Reynolds numbers

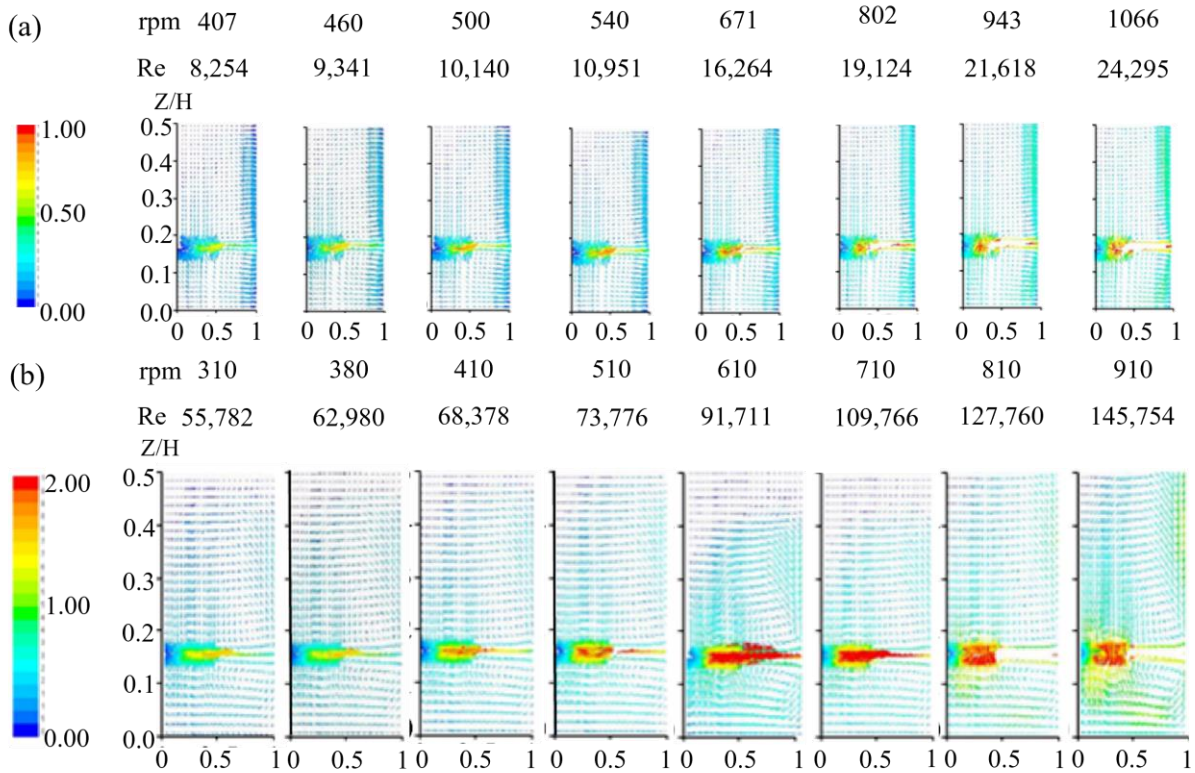

Fig. 13. The velocity vector plot of the disperse phase at the steady state of the small (a) and large (b) stirred tanks under various Reynolds numbers

Figure 14 depicts the effect of the Reynolds number on the radial distribution of the radial velocity of dispersed phase within the small (a) and large (b) reactors at heights z/H = 0.1 and 0.5 from the bottom of the tank. These dimensionless heights are located below and above the impeller, respectively. A positive velocity represents the fluid moving from the agitator to the wall, whereas a negative velocity represents the fluid moving from the wall to the agitator. At z/H = 0.1, negative radial velocities are observed in small and large stirred tanks, indicating that the fluid moves backward from the wall to the center of the tank. At z/H = 0.5, most of the fluid flows backwards from the wall to the center of the tank. However, a positive velocity is observed near the center of the large tank, indicating the fluid returning to the impeller. Increasing the Reynolds number results in a uniform radial distribution of the radial velocity.

Figure 15 shows the radial distribution of the axial velocity in the small and large stirred tanks for various Reynolds numbers. Positive and negative magnitudes represent upward and downward flows, respectively. At z/H = 0.1, two regions of fluid flow are observed, wherein the fluid flows upward in the center region and downward in the annular region. This flow pattern represents fluid recirculated from the annulus to the center of the tank. In addition, the annular region of the small tank is greater than that of the large tank because of the high wall frictional effect. At z/H = 0.5, a contrasting trend is observed, wherein the fluid flows upward in the annular region and downward in the center region, representing the recirculation of the fluid in the upper region. However, the annular regions of the small and large tanks are not significantly different (0.85 < r/R < 1.0). The free space above the liquid layer potentially decreases the effect of wall friction on the fluid flow in the annular region. The high axial velocity magnitude near the center and the wall regions is consistent with that observed experimentally using LDA [16]. In addition, the uniformity of the radial distribution decreases with increasing Reynolds number.

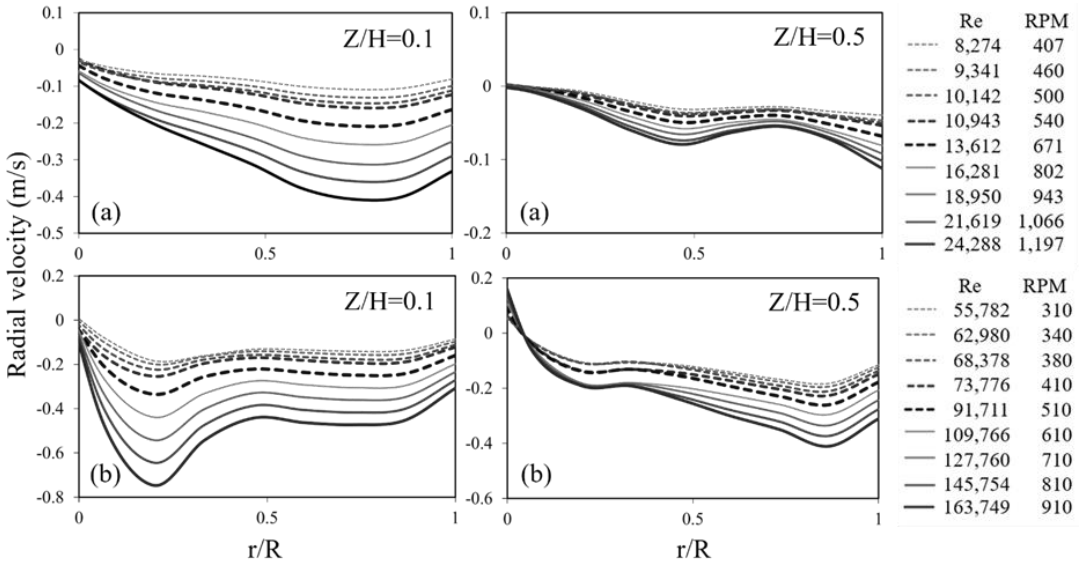

Fig. 14. The effect of the Reynolds number on the radial distribution of the radial velocity of dispersed phase within the small reactor (a) and large reactor (b) at the height Z/H = 0.1 and 0.5 above the tank bottom

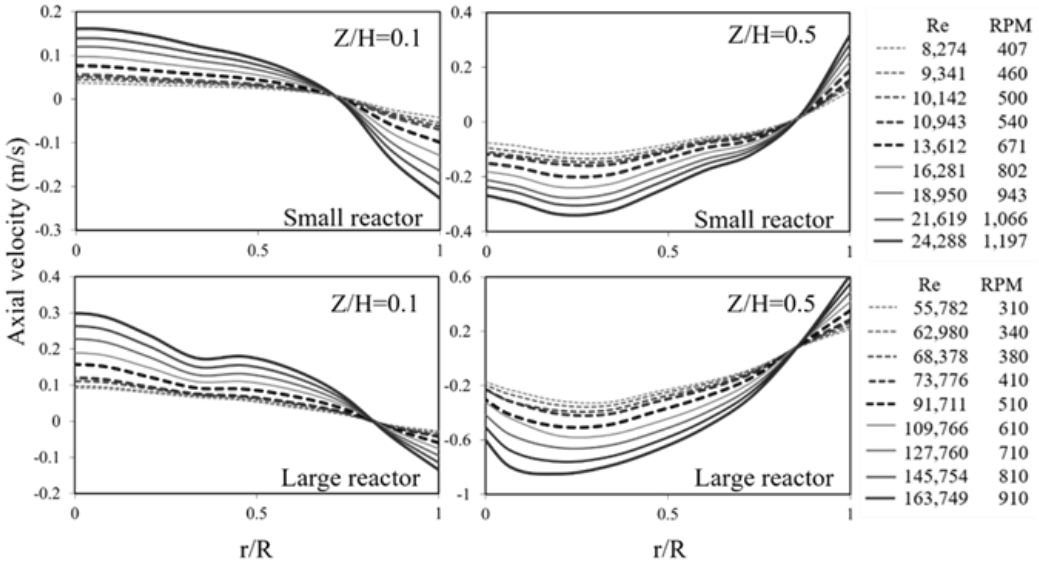

Fig. 15. The effect of the Reynolds number on the radial distribution of the axial velocity of dispersed phase within the small reactor (a) and large reactor (b) at the height Z/H = 0.1 and 0.5 above the tank bottom

Figure 16 shows the radial distribution of the tangential velocity. A positive velocity represents the liquid moving clockwise, and a negative velocity represents counterclockwise motion. The reactor size significantly affects the tangential velocity profile. At z/H = 0.1, the tangential velocity at the center is low because the fluid moves upward (Figure 11). A uniform distribution is obtained for the small tank. In the large stirred tank, the tangential velocity profile is non-uniform, particularly at high rotational speeds. The maximum velocity magnitude is observed at r/R = 0.8. At z/H = 0.5, the magnitude of the tangential velocity tends to increase with the radial position of the small tank. For the large stirred tank, two minimum peaks at r/R = 0.2 and 0.9 are observed.

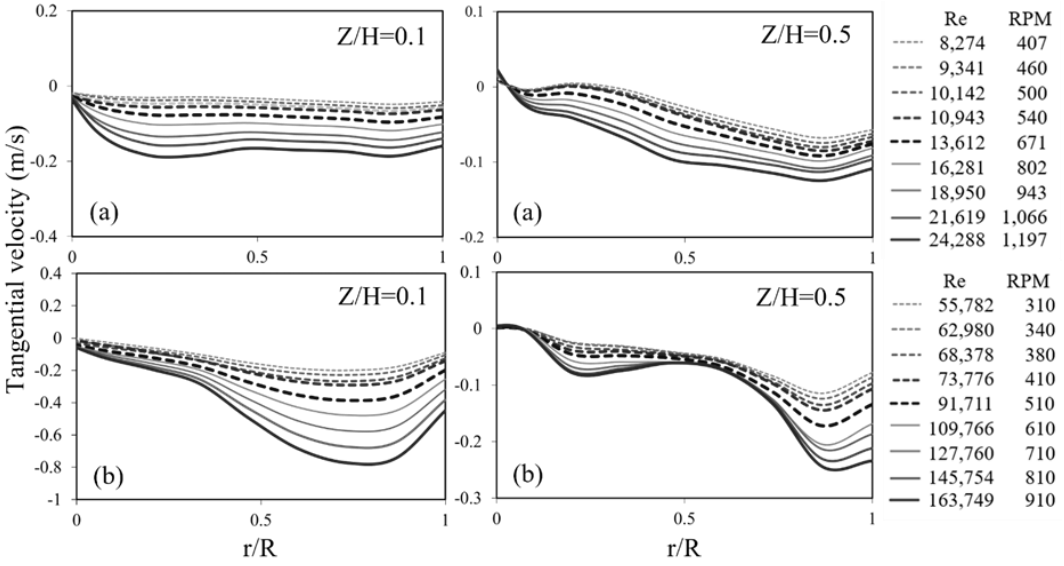

Fig. 16. The effect of the Reynolds number on the radial distribution of the tangential velocity of dispersed phase within the small reactor (a) and large reactor (b) at the height Z/H = 0.1 and 0.5 above the tank bottom

3.4 Tip Velocity and Mixing Time

Figure 17 demonstrates the effect of the Reynolds number on the tip velocities of the small and large stirred tanks. The tip velocity tends to increase with increasing Reynolds number owing to a simultaneous increase in the stirring speed. Although a large stirred tank is operated at a lower stirring speed than that of a small stirred tank, its large angular velocity generates a high tip velocity. In addition, the tip velocity of the small stirred tank is more sensitive to the Reynolds number than that of the large stirred tank.

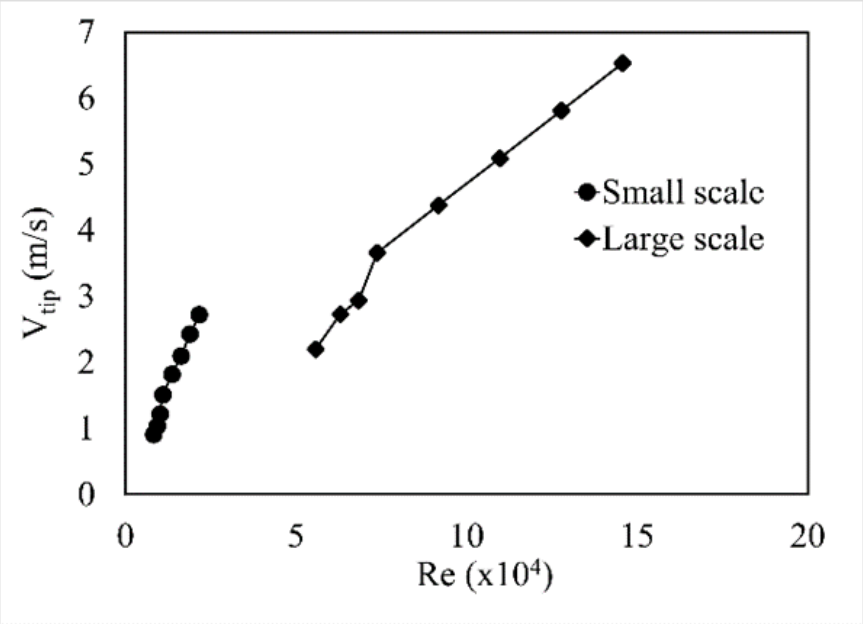

Fig. 17. The effect of Reynolds number on the tip velocity of the small and large stirred tanks

For immiscible liquid reactions, mass transfer resistance significantly affects overall reactor performance. The mixing performance was characterized by the mixing time (t_{mix}). Figure 18 indicates the effect of the Reynolds number on the mixing time in the small and large stirred tanks. In the small tank, the mixing time substantially decreases with increasing Reynolds number because of the high impeller speed. In the large stirred tank, the mixing time tends to decrease slightly with increasing Reynolds number and subsequently approaches a constant at a considerably high Reynolds number.

3.5 Scale Up of Stirred Tank

The reactor scale significantly affects the flow behavior in the stirred tank, as discussed in the previous section; thus, upscaling such reactors is difficult. A constant mixing time was chosen for this upscaling process. A upscaling law based on a single-phase liquid mixture proposed by Norwood and Metzner (1960) [39] was used in this study. The correlation can be written as,

$$N_L = N_S\left(\frac{T_S}{T_L}\right)^{1/4} = N_S\left(\frac{1}{3}\right)^{1/4} \quad (17)$$

where N is the impeller speed (rpm), and T is the tank diameter (m). The subscripts L and S represent large- and small-scale reactors, respectively.

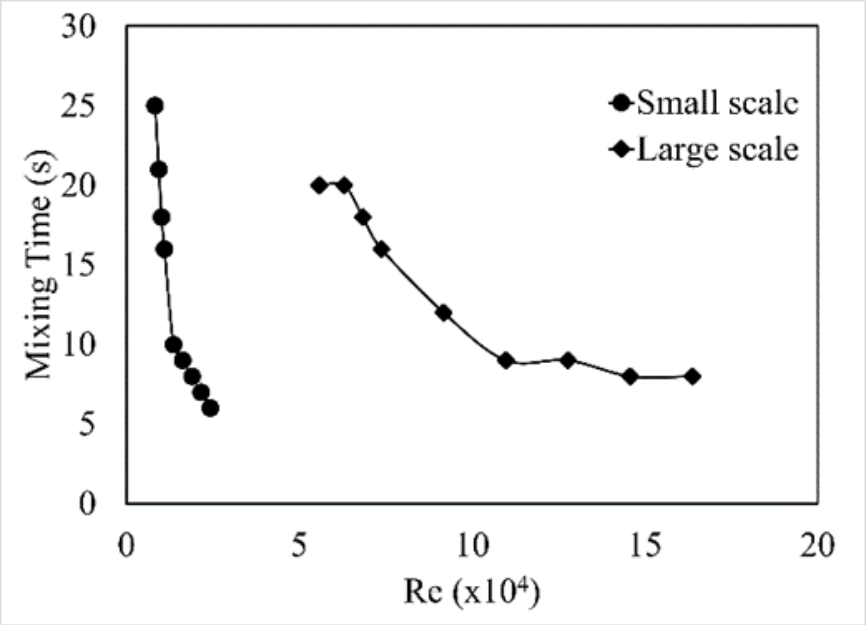

Fig. 18. the effect of Reynolds number on the mixing time in the small and large stirred tanks

Table 1 lists the impeller speeds of the small and large stirred tanks, corresponding to the proposed scaling law. Figure 19 depicts the parity plot of the mixing time in the small- and large-scale reactors using the Norwood and Metzner upscaling law. The mixing times of the small and large stirred tanks are similar, demonstrating a difference in the range of $\pm 10\%$. Therefore, the scaling law based on a single-phase liquid mixture can be effectively used to scale up an immiscible liquid–liquid stirred tank.

Table 1
The impeller speeds of the small and large stirred tanks corresponding to the proposed scaling law

Small tank reactor		Large tank reactor	
N_S	$Re\ (-)$	$N_L = 0.760N_s$	$Re\ (-)$
276	5,605	210	37,788
407	8,247	310	55,782
460	9,341	350	62,980
500	10,142	380	68,378
540	10,943	410	73,776
671	13,621	510	91,711
802	16,281	610	109,766
934	18,950	710	127,760
1066	21619	810	145,754
1197	24288	910	163,749

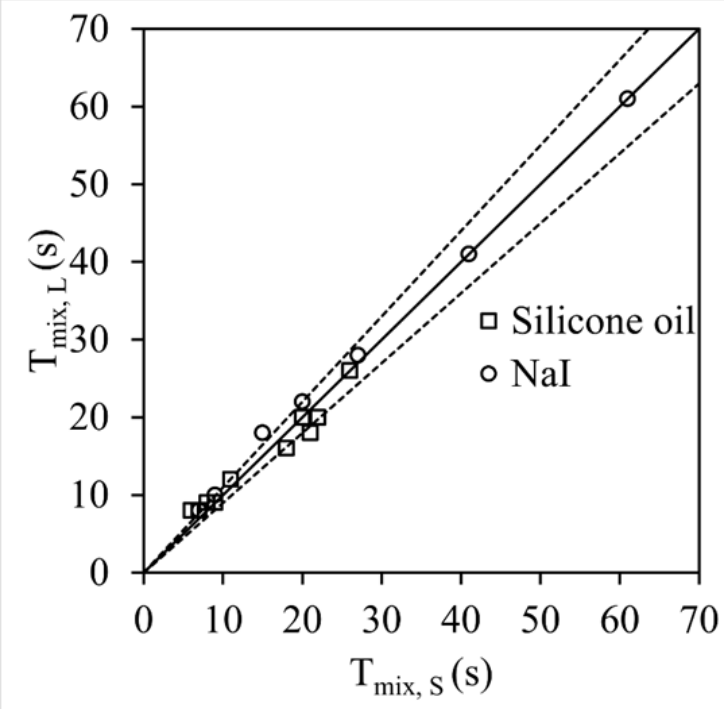

Fig. 19. The parity plot of the mixing time in a small- and large-scale reactors using Norwood and Metzner scaling law

4. Conclusions

Immiscible liquid–liquid stirred tanks are extensively used in various industries owing to their excellent heat and mass transfer. Upscaling such reactors is essential for industrial-scale production. However, the upscaling process is challenging, owing to the complexity of the flow behavior within the system. Thus, the objectives of this study were to investigate the flow behavior and upscale an immiscible liquid–liquid stirred tank using CFD simulations. A silicone oil–NaI solution was mixed in a flat-bottomed stirred tank reactor, equipped with a six-blade Rushton turbine, and subsequently analyzed. The hydrodynamic behavior was used to validate the CFD model. The simulated results were in good agreement with the experimental data. The operating conditions and reactor scale significantly impacted the hydrodynamic behavior. The velocity distribution became less uniform as the Reynolds number increased. Two reactor sizes with a tank diameter of 0.14 m (base size) and 0.42 m (three times larger than base size) were used for the upscaling study considering geometric similarity. The scaling law for a constant mixing time based on that of Norwood and Metzner (1960) was defined in the study. The proposed scaling law reliably scaled up the immiscible liquid–liquid mixing in a stirred tank with a difference in the range of $\pm 10\%$.

Acknowledgement
This research was funded by a grant from the Office of The Higher Education Commission under the instructor and personnel development project for higher education institutions in special development zones in the Southern border provinces, Thailand.

References

[1] Tadros, Tharwat F. "Emulsion formation, stability, and rheology." *Emulsion formation and stability* 1 (2013): 1-75. https://doi.org/10.1002/9783527647941.ch1

[2] Leng, Douglas E., and Richard V. Calabrese. "Immiscible liquid–liquid systems." *Handbook of Industrial Mixing: Science and Practice* 3952, no. 2006 (2004): 639-753. https://doi.org/10.1002/0471451452.ch12

[3] Fabio Laurenzi, Mirella Coroneo, Giuseppina Montante, Alessandro Paglianti, and Franco Magelli. "Experimental and computational analysis of immiscible liquid–liquid dispersions in stirred vessels." *Chemical Engineering Research and Design* 87, no. 4 (2009): 507-514. https://doi.org/10.1016/j.cherd.2008.12.007

[4] Mohd Izzudin Izzat Zainal Abidin, Abdul Aziz Abdul Raman, and Mohamad Iskandr Mohamad Nor. "Experimental Investigations in Liquid–Liquid Dispersion System: Effects of Dispersed Phase Viscosity and Impeller Speed." *Industrial & Engineering Chemistry Research* 53, no. 15 (2014): 6554-6561. https://doi.org/10.1021/ie5002845

[5] Piero M. Armenante, Changgen Luo, Chun-Chiao Chou, Ivan Fort, and Jaroslav Medek. "Velocity profiles in a closed, unbaffled vessel: comparison between experimental LDV data and numerical CFD predictions." *Chemical Engineering Science* 52, no. 20 (1997): 3483-3492. https://doi.org/10.1016/S0009-2509(97)00150-4

[6] Dang Cheng, Jingcai Cheng, Yumei Yong, Chao Yang, and Zaisha Mao. "CFD Prediction of the Critical Agitation Speed for Complete Dispersion in Liquid-Liquid Stirred Reactors." *Chemical Engineering & Technology* 34, no. 12 (2011): 2005-2015. https://doi.org/10.1002/ceat.201100220

[7] Adnan Ghulam Mustafa, Mohd Fadhil Majnis, and Nor Azyati Abdul Muttalib. "CFD Study on Impeller Effect on Mixing in Miniature Stirred Tank Reactor." *CFD Letters* 12, no. 10 (2020): 15-26. https://doi.org/10.37934/cfdl.12.10.1526

[8] Suzanne M. Kresta, Deming Mao, and Vesselina Roussinova. "Batch blend time in square stirred tanks." *Chemical Engineering Science* 61, no. 9 (2006): 2823-2825. https://doi.org/10.1016/j.ces.2005.10.069

[9] Suci Madhania, Tantular Nurtono, Anugrah Budi Cahyani, Yuswan Muharam, Sugeng Winardi, and Widodo Wahyu Purwanto. "Mixing behaviour of miscible liquid-liquid multiphase flow in stirred tank with different marine propeller installment by computational fluid dynamics method." *Chemical Engineering Transactions* 56 (2017): 1057-1062.

[10] Ian TorotwaChangying Ji. "A Study of the Mixing Performance of Different Impeller Designs in Stirred Vessels Using Computational Fluid Dynamics." *Designs* 2, no. 1 (2018): 10. https://doi.org/10.3390/designs2010010

[11] Francesco Maluta, Giuseppina Montante, and Alessandro Paglianti. "Analysis of immiscible liquid-liquid mixing in stirred tanks by Electrical Resistance Tomography." *Chemical Engineering Science* 227 (2020): 115898. https://doi.org/10.1016/j.ces.2020.115898

[12] Nurul Farhana Mohd Yusof, Edmund Ung Eng Soon, Iman Fitri Ismail, and Akmal Nizam Mohammed. "Mixing Performance of Anchor and Helical Stirrer Blades for Viscous Fluid Applications." *CFD Letters* 13, no. 1 (2021): 58-71. https://doi.org/10.37934/cfdl.13.1.5871

[13] A. Giapos, Chrysostomos Pachatouridis, and Michael Stamatoudis. "Effect of the Number of Impeller Blades on the Drop Sizes in Agitated Dispersions." *Chemical Engineering Research & Design* 83 (2005): 1425-1430. https://doi.org/10.1205/cherd.04167

[14] Francis X. McConvilleStephen B. Kessler, *Scale-Up of Mixing Processes: A Primer*, in *Chemical Engineering in the Pharmaceutical Industry*, D.J. am-Ende, Editor. 2010. p. 249-267. https://doi.org/10.1002/9780470882221.ch14

[15] Hugo A. Jakobsen, *Agitation and Fluid Mixing Technology*, in *Chemical Reactor Modeling: Multiphase Reactive Flows*. 2014, Springer International Publishing: Cham. p. 809-881. https://doi.org/10.1007/978-3-319-05092-8_7

[16] Jan-Erik SvenssonAnders Rasmuson. "LDA-Measurements in a Stirred Tank With a Liquid-Liquid System at High Volume Percentage Dispersed Phase." *Chemical Engineering & Technology* 27 (2004): 335-339. https://doi.org/10.1002/ceat.200401981

[17] Nelvin Kaw Chee Qing, Nor Afzanizam Samiran, and Razlin Abd Rashid. "CFD Simulation analysis of Sub-Component in Municipal Solid Waste Gasification using Plasma Downdraft Technique." *Journal of Advanced Research in Numerical Heat Transfer* 8, no. 1 (2022): 36-43.

[18] Nor Azwadi Che Sidik, Solihin Musa, Siti Nurul Akmal Yusof, and Erdiwansyah Erdiwansyah. "Analysis of Internal Flow in Bag Filter by Different Inlet Angle." *Journal of Advanced Research in Numerical Heat Transfer* 3, no. 1 (2020): 12-24.

[19] Samsudin Anis, Shilly Muttashillatul Urfi, Adhi Kusumastuti, and Wim Widyo Baskoro. "Analysis of Inlet Temperature and Airflow Rate on Drying Process in a Spray Dryer Using Computational Fluid Dynamics Method." *Journal of Advanced Research in Fluid Mechanics and Thermal Sciences* 94, no. 1 (2022): 163-171. https://doi.org/10.37934/arfmts.94.1.163171

[20] Arina Mohd Noh, Sohif Mat, and Mohd Hafidz Ruslan. "CFD Simulation of Temperature and Air Flow Distribution inside Industrial Scale Solar Dryer." *Journal of Advanced Research in Fluid Mechanics and Thermal Sciences* 45, no. 1 (2018): 156-164.

[21] Thineshwaran SubramaniamMohammad Rasidi Rasani. "Pulsatile CFD Numerical Simulation to investigate the effect of various degree and position of stenosis on carotid artery hemodynamics." *Journal of Advanced Research in Applied Sciences and Engineering Technology* 26, no. 2 (2022): 29-40. https://doi.org/10.37934/araset.26.2.2940

[22] Parinya Khongprom, Supawadee Ratchasombat, Waritnan Wanchan, Panut Bumphenkiattikul, and Sunun Limtrakul. "Scaling of a catalytic cracking fluidized bed downer reactor based on computational fluid dynamics simulations." *RSC Advances* 10, no. 5 (2020): 2897-2914. https://doi.org/10.1039/C9RA10080F
[23] Vivek V. Ranade, *10 Stirred Reactors*, in *Process Systems Engineering*, V.V. Ranade, Editor. 2002, Academic Press. p. 285-325. https://doi.org/10.1016/S1874-5970(02)80011-X
[24] Feng WangZai-Sha Mao. "Numerical and Experimental Investigation of Liquid−Liquid Two-Phase Flow in Stirred Tanks." *Industrial & Engineering Chemistry Research* 44, no. 15 (2005): 5776-5787. https://doi.org/10.1021/ie049001g
[25] Gopal R. Kasat, Avinash R. Khopkar, Vivek Ranade, and Aniruddha Bhalchandra Pandit. "CFD simulation of liquid-phase mixing in solid–liquid stirred reactor." *Chemical Engineering Science* 63, no. 15 (2008): 3877-3885. https://doi.org/10.1016/j.ces.2008.04.018
[26] Milan Jahoda, L. Tomášková, and Michal Moštěk. "CFD Prediction of Liquid Homogenisation in a Gas–Liquid Stirred Tank." *Chemical Engineering Research & Design* 87 (2009): 460-467. https://doi.org/10.1016/j.cherd.2008.12.006
[27] Gaurav MittalRafael Issao Kikugawa. "Computational fluid dynamics simulation of a stirred tank reactor." *International Conference on Technological Advancements in Materials Science and Manufacturing* 46 (2021): 11015-11019. https://doi.org/10.1016/j.matpr.2021.02.102
[28] Widiawaty Candra Damis, Siswantara Ahmad Indra, R. Gunadi Gun Gun, Andira Mohamad Arif, Budiarso, Budiyanto Muhammad Arif, M. Hilman Gumelar Syafei, and Adanta Dendy. "Optimization of inverse-Prandtl of Dissipation in standard k-ε Turbulence Model for Predicting Flow Field of Crossflow Turbine." *CFD Letters* 14, no. 1 (2022): 112-127. https://doi.org/10.37934/cfdl.14.1.112127
[29] L. Dong, Stein Tore Johansen, and Thorvald Abel Engh. "Flow induced by an impeller in an unbaffled tank—I. Experimental." *Chemical Engineering Science* 49, no. 4 (1994): 549-560. https://doi.org/10.1016/0009-2509(94)80055-3
[30] L. Dong, Stein Tore Johansen, and Thorvald Abel Engh. "Flow induced by an impeller in an unbaffled tank—II. Numerical modelling." *Chemical Engineering Science* 49, no. 20 (1994): 3511-3518. https://doi.org/10.1016/0009-2509(94)00150-2
[31] Mohammad Hassan VakiliMohsen Nasr Esfahany. "CFD analysis of turbulence in a baffled stirred tank, a three-compartment model." *Chemical Engineering Science* 64, no. 2 (2009): 351-362. https://doi.org/10.1016/j.ces.2008.10.037
[32] Zhaoyou Zhu, Bin Qin, Shuhua Li, Yigang Liu, Xin Li, Peizhe Cui, Yinglong Wang, and Jun Gao. "Multi-dimensional analysis of turbulence models for immiscible liquid-liquid mixing in stirred tank based on numerical simulation." *Separation Science and Technology* 56, no. 2 (2021): 411-424. https://doi.org/10.1080/01496395.2020.1715436
[33] Aoyi OchiengMaurice Onyango. "CFD simulation of the hydrodynamics and mixing time in a stirred tank." *Chemical Industry and Chemical Engineering Quarterly* 16, no. 4 (2010): 379-386. https://doi.org/10.2298/CICEQ100211040O
[34] Dang Cheng, Xin Feng, Jingcai Cheng, and Chao Yang. "Numerical simulation of macro-mixing in liquid–liquid stirred tanks." *Chemical Engineering Science* 101 (2013): 272-282. https://doi.org/10.1016/j.ces.2013.06.026
[35] Giuseppina Montante, Michal Moštěk, Milan Jahoda, and Franco Magelli. "CFD simulations and experimental validation of homogenisation curves and mixing time in stirred Newtonian and pseudoplastic liquids." *Chemical Engineering Science* 60, no. 8-9 (2005): 2427-2437. https://doi.org/10.1016/j.ces.2004.11.020
[36] Nandkishor K. Nere, Ashwin W. Patwardhan, and Jyeshtharaj B. Joshi. "Liquid-Phase Mixing in Stirred Vessels: Turbulent Flow Regime." *Industrial & Engineering Chemistry Research* 42, no. 12 (2003): 2661-2698. https://doi.org/10.1021/ie0206397
[37] Fah Al-QaessiLaila Abu-Farah. "Prediction of Mixing Time for Miscible Liquids by CFD Simulation in Semi-Batch and Batch Reactors." *Engineering Applications of Computational Fluid Mechanics* 3, no. 1 (2009): 135-146. https://doi.org/10.1080/19942060.2009.11015260
[38] Zied Driss, Ahmed Kaffel, Bilel Ben Amira, Ghazi Bouzgarrou, and Mohamed Salah Abid. "PIV Measurements to Study the Effect of the Reynolds Number on the Hydrodynamic Structure in a Baffled Vessel Stirred by a Rushton Turbine." *American Journal of Energy Research* 2, no. 3 (2014): 67-73. https://doi.org/10.12691/ajer-2-3-4
[39] K. W. NorwoodArthur B. Metzner. "Flow patterns and mixing rates in agitated vessels." *Aiche Journal* 6 (1960): 432-437. https://doi.org/10.1002/aic.690060317